J Appl Electrochem (2009) 39:899–906
DOI 10.1007/s10800-008-9735-8

ORIGINAL PAPER

Effect of oxidation on the performance of low-temperature petroleum cokes as anodes in lithium ion batteries

A. Concheso · R. Santamaría · R. Menéndez · J. M. Jiménez-Mateos · R. Alcántara · G. F. Ortiz · P. Lavela · J. L. Tirado

Received: 9 April 2008 / Accepted: 24 November 2008 / Published online: 17 December 2008

Abstract The effect of an oxidative treatment on the electrochemical performance of various low-temperature cokes as anodes in lithium ion batteries was examined in order to optimize their chemical composition and textural properties. Annealing in a stream of dry synthetic air over short time and temperature ranges was found to result in substantially increased cell capacity and improved capacity retention during cycling in coke oxidized at 350 °C for 1 h, which exhibited a capacity as high as 385 mAh g^{-1} after 20 cycles at C/50. However, raising the oxidation temperature to 500 °C resulted in undesirably increased irreversible capacity and polarization between the charge and discharge branches, the effect being confirmed by the high impedance values obtained after only a few cycles. ^{7}Li MAS NMR spectroscopy was used to assess covalency in lithium bonds and its relationship to electrochemical performance in the studied batteries.

Keywords Lithium · Coke · Oxidation · Battery

1 Introduction

Coke is a by-product of the petroleum industry. The low cost of this carbonaceous material and its ability to react with large amounts of lithium have promoted vast efforts towards obtaining high-performance coke-based anode materials for use in lithium ion batteries [1–4]. Unlike graphitized materials, where lithium insertion between graphene layers is the dominant mechanism, the electrochemical reaction of lithium with cokes occurs on the solid electrode surface. The outcome of the electrochemical reaction is influenced by the presence of functionalized organic groups and/or dangling bonds at the edge planes of graphene layers. These organic groups tend to react irreversibly with lithium and result in irreversible capacity losses and high polarization on cycling. This problem has been addressed in various ways involving strict control of the carbonization temperature [5], particle morphology [6] and presence of heteroatoms [7]. Also, nanostructuring has provided new, mechanically or chemically modified carbon materials with improved properties as electrodes [8, 9].

Recent achievements in the preparation of new carbonaceous materials with better electrochemical properties as anodes in Li-ion batteries testify to the significance of surface chemistry in this field [10, 11]. Thus, mild oxidation of carbon surfaces has proved an effective chemical method for obtaining graphitized materials with improved properties as electrodes in lithium cells [12–14]. The oxidation procedure facilitates removal of highly reactive imperfections leading to irreversible reaction with lithium, as well as the formation of a dense layer of oxides. Moreover, oxidation is intended to inhibit decomposition of the electrolyte and create pores and nanocavities for lithium insertion. Both effects are believed to facilitate long-term cycling of lithium cells. Using oxidative chemical procedures with low-temperature carbon materials may open up new prospects for their use in advanced electrochemical systems. Thus, a net improvement in performance in oxidized carbons was recently demonstrated by using hydrogen peroxide as oxidant [15].

A. Concheso · R. Santamaría · R. Menéndez
Instituto Nacional del Carbón, CSIC, Apartado 73, 33080 Oviedo, Spain

J. M. Jiménez-Mateos
REPSOL YPF, Ctra. N-V km 18, 28930 Mostoles, Madrid, Spain

R. Alcántara · G. F. Ortiz · P. Lavela (✉) · J. L. Tirado
Laboratorio de Química Inorgánica, Universidad de Córdoba, Campus de Rabanales, 14071 Cordoba, Spain
e-mail: iq1lacap@uco.es

In this work, a straightforward, inexpensive oxygen-based oxidation procedure was applied to by-products of the petroleum industry to obtain high added value materials potentially useful as anodes for lithium-ion batteries.

2 Experimental

Three green petroleum coke samples were provided by REPSOL YPF. The raw materials were carbonized at 800 °C under a N_2 stream. The resulting products were designated S1, S2 and S3. The temperature used was chosen from previous experience with these carbonaceous materials as the optimum compromise between irreversible and reversible capacities [15]. The carbonized cokes were then heated at 400 °C under a flowing stream of synthetic air at 40 L h^{-1} for 3 h. Coke S1 was additionally heated at 350 °C for 1 h and 500 °C for 3 h.

The carbon, hydrogen, nitrogen and sulphur contents of the cokes were determined with a LECO-CHNS-932 elemental analyser, and the oxygen content on a LECO-VTF-900 graphite furnace. XRD patterns were recorded on a Siemens D-5000 instruments using CuKα radiation. Carbon densities were measured with an AccuPyc 1330 helium pycnometer.

Electrochemical tests were performed with two- and three-electrode Swagelok-type lithium cells. The counter and reference electrodes were both 9 mm discs of lithium metal, and the working electrode consisted of a mixture of 92% active material and 8% PVDF binder coating a piece of copper foil of identical diameter. The electrolyte solution, 1 M $LiPF_6$ (EC:DE = 1:1), was supported on Whatman glass fibre discs. An Arbin potentiostat/galvanostat multi-channel system was used to cycle two electrode lithium cells at C/50 for both the charge and discharge branch. An Autolab PGSTAT12 system was used for Electrochemical Impedance Spectroscopy (EIS) measurements. To this end, three-electrode lithium cells were successively cycled by passing a current between the working electrode (coke sample) and counter electrode (Li). The impedance spectra for the carbon electrode were recorded against a Li reference electrode; the test cells were allowed to relax at open circuit for at least 5 h to ensure *quasi*-equilibrium. An AC voltage signal of 5 mV was applied from 100 kHz to 3 mHz.

^{7}Li NMR spectra were recorded on an Avance 400WD solid-state spectrometer (155.4 MHz resonance frequency for ^{7}Li) with magic-angle spinning (12 kHz). Line shifts were measured with respect to LiCl as external standard. Discharged electrodes were rinsed with propylene carbonate, dried in vacuum and placed in a tightly closed NMR sample holder under an argon atmosphere.

3 Results and discussion

The chemical composition of the coke samples, carbonized at 800 °C, is shown in Table 1. Their hydrogen contents decreased slightly from S1 to S3. S1 exhibited the lowest contents in N and S. On the other hand, S3 contained nearly 6% sulphur. BET surface areas were all rather low (1–3 m^2 g^{-1}); this is a desirable feature for carbonaceous materials to be used as electrodes in lithium batteries as it can help avoid excessive electrolyte decomposition during battery discharge.

The XRD patterns for the carbonized coke samples, not shown, exhibited two main broadened reflections (002 and 110) corresponding to a highly turbostratic structure typical of disordered carbons [8]. Neither the thermal treatment nor chemical oxidation induced any clearly apparent changes in turbostratic character.

The optical texture of the cokes carbonized at 800 °C can be ascribed to the nature of petroleum residua (particularly, their chemical composition). In fact, composition strongly affects the reactivity, viscosity and, ultimately, coalescence in the mesophase, which dictates the final texture. The high sulphur content of S3 must have resulted from the presence of aliphatic chains, which create a highly reactive medium where viscosity rapidly increases during pyrolysis. This prevents mesogenic molecules from adopting an appropriate orientation and leads to the formation of the typical mosaic texture. In fact, S3 exhibited small mosaic domains. S2 and S1, which had a lower content in this heteroelement, exhibited larger flow domains (Fig. 1)

Lithium cells prepared from the original and air-oxidized cokes as working electrodes were subjected to galvanostatic cycling. Figure 2 shows their electrochemical profiles as plots of cell voltage versus composition and differential capacity versus cell voltage. A typical *quasi*-plateau corresponding to the SEI formation was observed at around 1 V during the first discharge. The irreversible character of this electrochemical deposition was strongly dependent on the heteroatom content of the coke and was responsible for an inevitable capacity loss relative to the next cycle. However, the chemical deposition of a stable, conductive interface facilitates growth of a passivating layer during the first discharge which does not hinder lithium migration during subsequent cycling [16, 17]. A comparison of the curves in Fig. 2 reveals an increased

Table 1 Chemical composition of the carbonized cokes

	C (%)	H (%)	N (%)	S (%)	O (%)
S1	97.61	0.88	0.16	0.05	1.30
S2	95.96	0.80	1.84	0.35	1.05
S3	91.96	0.72	1.47	5.06	0.79

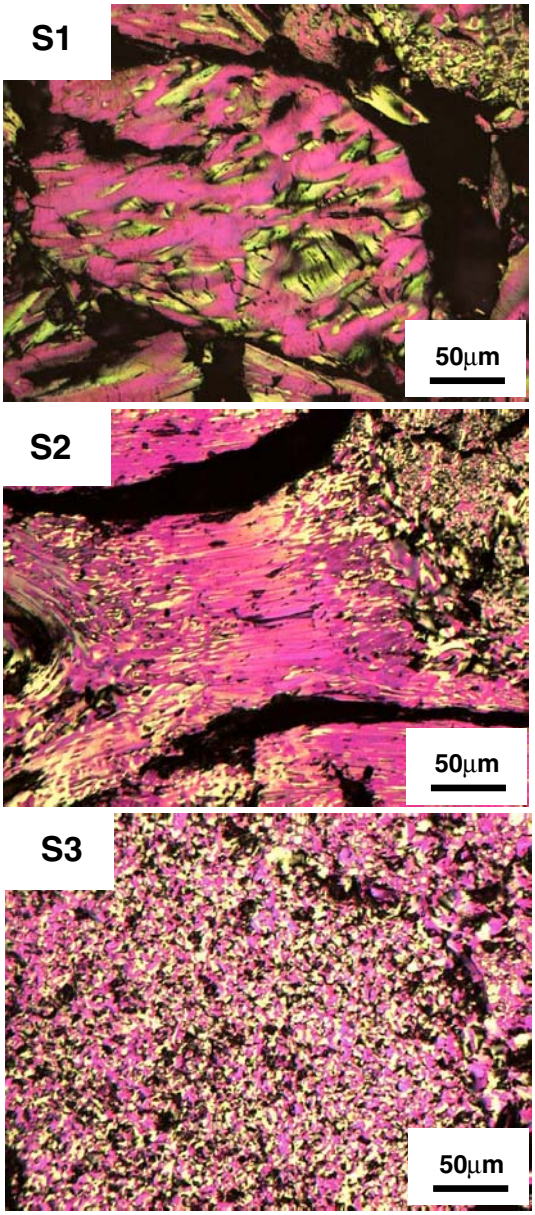

Fig. 1 Optical texture of S1, S2 and S3 cokes

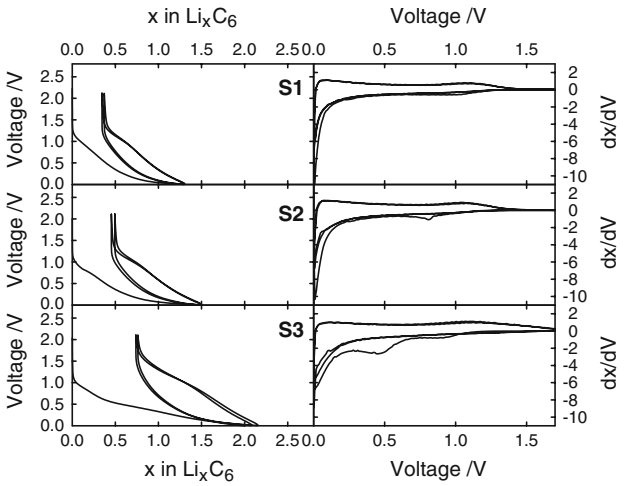

Fig. 2 Voltage versus composition and differential capacity versus voltage charge/discharge obtained by the galvanostatic method of untreated cokes. Kinetic rate: C/10

irreversible capacity in S2 and S3. This is reflected in the 2presence of irreversible bands in the d*x*/d*V* vs. *V* plots at ca. 0.8 V for S2 and ca. 0.5 V for S3. These signals had previously been assigned to heteroelements reacting irreversibly with Li [18, 19]. In recent studies, we found this detrimental effect of sulphur to be effectively suppressed by using a chemical pretreatment to obtain metal/carbon composites. Thus, metal atoms react with sulphur to form sulphides which hinder lithium trapping and provide the electrode material with reversible capacity via a conversion reaction [20].

On subsequent cycling, we found the broadened band at ca. 1 V to be partially retained. This may has been a result of lithium reacting with hydrogen atoms in surface groups. This reaction is deemed partially reversible and responsible for the significant polarization of the electrochemical curve observed upon charging, an effect which has been extensively verified in hard carbons [4]. Below 0.5 V, the cell voltage decreases more steadily, to final cut-off value at 0 V. At these potentials, lithium ions can be expected to react reversibly with coke. Lithium insertion in the highly distorted interlayer space of the poorly crystalline graphene layer, and the existence of alternative mechanisms for the lithium reaction via non-equivalent positions on carbon surfaces and particle edges, are responsible for the absence of the horizontal plateau typically observed in the profile for graphite.

Cokes are more reactive to air than are graphitized materials, so their thermal treatments can be done at lower temperatures [21]. In order to find the most suitable oxidation temperature, the carbonized coke was previously subjected to a thermal study. Thus, the weight loss of samples oxidized at 450, 500 and 550 °C was monitored for an extended period of time (Fig. 3). The large weight loss observed at 550 °C reflects uncontrolled sample combustion. For this reason, treatment temperatures above 500 °C were avoided.

Oxidation with air at 400 °C for 3 h caused a significant increase in oxygen content in all samples, but only minor changes in N, S and H (Table 2). The increase was more marked in S2 and S3, which possessed the highest heteroatom contents. Most probably, N and S atoms on the carbon surface with incomplete valence shells were readily oxidized and tended to adsorb greater amounts of oxygen as a result. Also, the smaller were the domains, the more abundant were reactive edge planes. The oxidation process caused significant changes in the electrochemical profiles (Fig. 4) including an increase in irreversibility during the

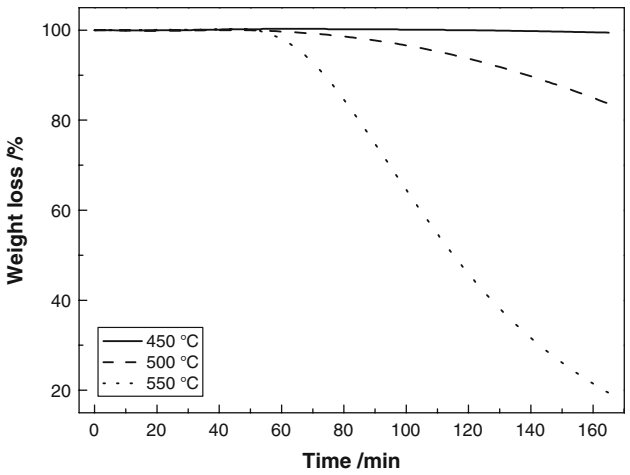

Fig. 3 TG curves of the oxidation reaction

Table 2 Chemical composition of the oxidized cokes

	C (%)	H (%)	N (%)	S (%)	O (%)
Oxidized S1 (400 °C, 3 h)	94.08	0.86	0.45	0.06	4.55
Oxidized S2 (400 °C, 3 h)	91.93	0.90	1.82	0.34	5.01
Oxidized S3 (400 °C, 3 h)	84.15	0.96	1.71	4.22	8.95
Oxidized S1 (350 °C, 1 h)	97.21	0.84	0.30	0.04	1.61
Oxidized S1 (500 °C, 3 h)	77.57	2.19	0.05	–	20.19

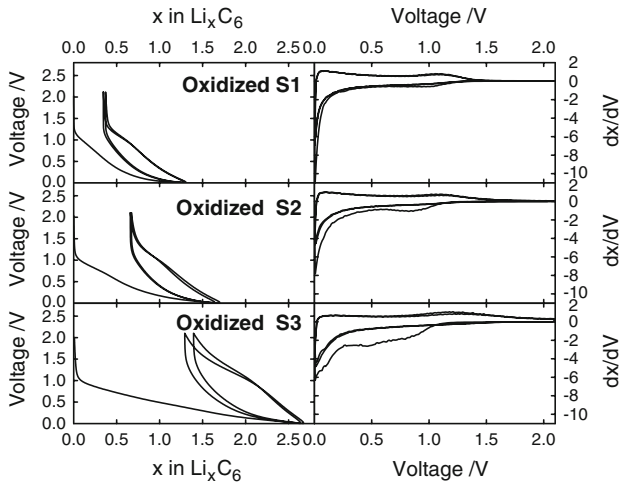

Fig. 4 Voltage versus composition and differential capacity versus voltage charge/discharge plots, obtained by the galvanostatic method, of oxidized cokes. Kinetic rate: C/10

first discharge. The effect increased with increasing content in heteroatoms. Thus, sample S1, which had the lowest content, exhibited no significant changes in its charge or discharge curves. By contrast, S2 and S3 exhibited an expansion of the irreversible region to values beyond $x = 0.5$. The linear relationship between the heteroelement content and irreversible capacity in the first cycle in both

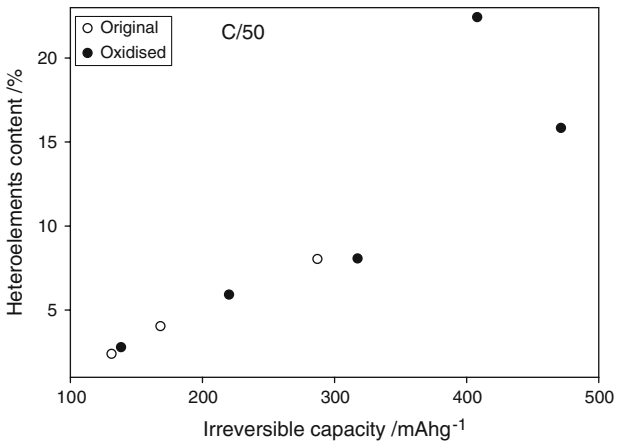

Fig. 5 Plot of the irreversible capacity in the first cycle versus heteroelement content (including overall composition of H, N, S and O)

the original and oxidized cokes is clearly apparent from Fig. 5, excepting for the sample oxidized at 500 °C. The huge increase in the irreversible capacity can be related with the strong adsorption of oxygen (Table 2). Likely, an excess of oxygen atoms on the carbon surface may favor lithium trapping and the growth on an excessively thick and less permeable SEI film that hampers lithium migration from the electrolyte into the carbon particle.

The results of galvanostatic cycling are illustrated in Fig. 6, which also shows those provided by lithium cells made from the original or oxidized cokes for comparison. Electrochemical performance was not so closely related to heteroelement contents over a large number of cycles. S2 exhibited the strongest capacity fading. Also, while oxidation with air had virtually no effect on S3, it substantially raised the capacity of S1. As confirmed by impedance measurements, this effect was mainly associated to the kinetic response of the carbonaceous materials.

Electrochemical impedance spectroscopy has proved a useful tool for unravelling interfacial phenomena influencing the kinetic behaviour of carbon materials [22]. Figure 7 shows Nyquist plots for the original and oxidized cokes after the first, third and 10th discharge. Values were mass-normalized for easier comparison. The equivalent circuit used to fit the experimental data is described elsewhere [6]. Resistances R_{SL} and R_{CT} were calculated from the diameters of the two depressed semi-circles observed at high and medium frequencies. These parameters are usually assigned to the resistance to lithium migration through the electrolyte interface (SEI) and insertion reaction in the bulk medium, respectively. Using a constant phase element, Q, instead of a capacitor allows the depression of the semi-circles to be considered. The straight line obtained at low frequencies, which was fitted to a Warburg component (W), describes the system response to Li^+ diffusion through intercalated carbon.

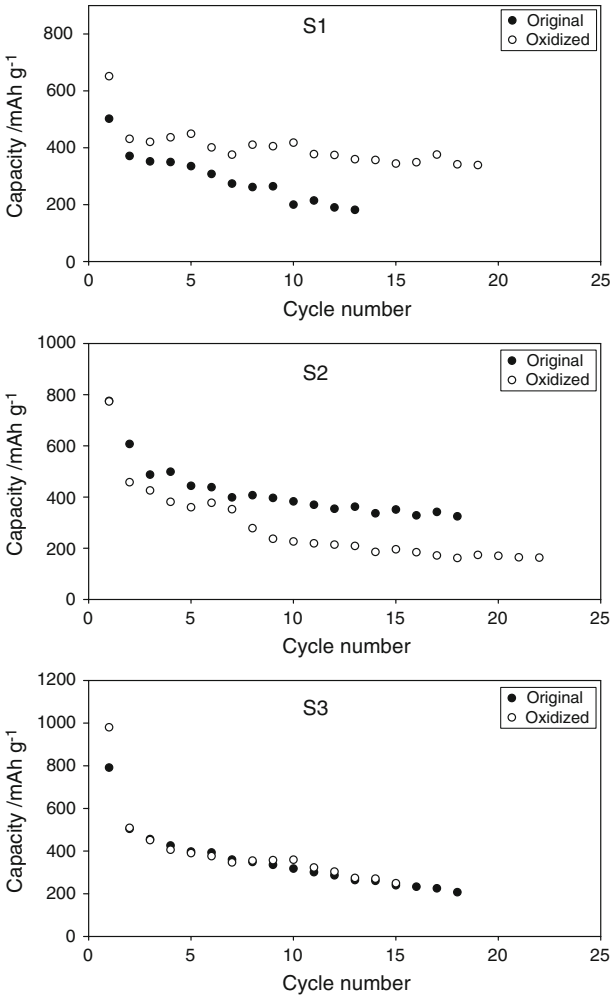

Fig. 6 Galvanostatic cycling of untreated and oxidized cokes at C/50

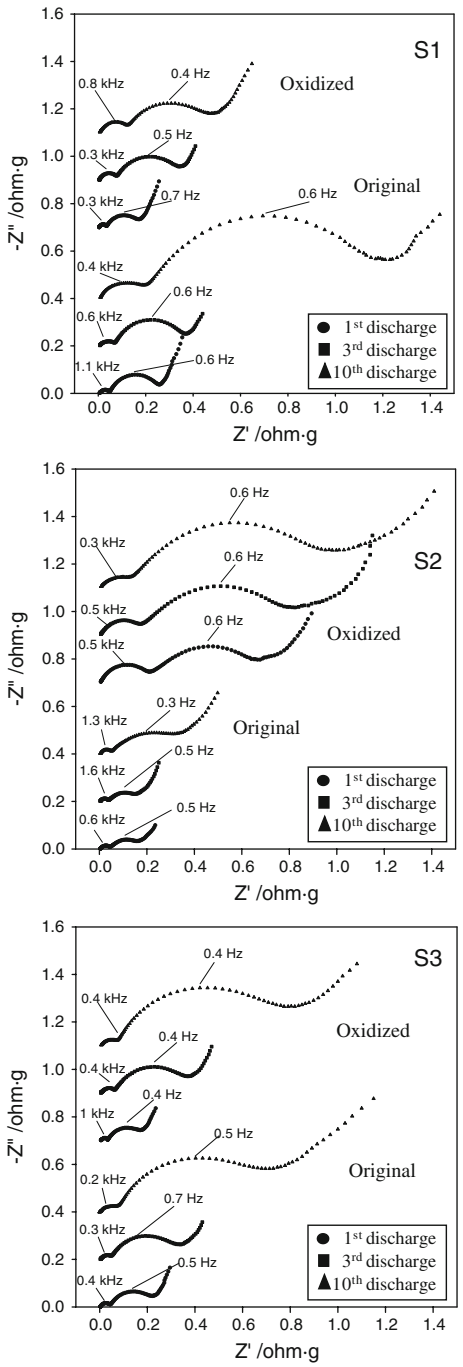

Fig. 7 Nyquist plots of three-electrode lithium cells assembled with untreated and oxidized cokes at the end of the first, third and 10th discharge

The spectra for S2 revealed an abrupt increase in R_{SL} and R_{CT} on cycling; by contrast, S3 exhibited negligible changes in both parameters. This is quite consistent with the above-described electrochemical performance. Thus, the increased resistance of oxidized S2 was the main source of its poor performance. In original S1, R_{CT} after the tenth discharge increased more abruptly than it did in the oxidized sample. This is consistent with the capacity fading in the former sample when used as electrode material in the lithium test cells.

Because S1 proved the most efficient coke for the intended purpose, it was selected for further study of the oxidation variables. Thus, the coke was oxidized at variable temperatures and for variable lengths of time. As expected, the moderate decrease in both parameters in the sample treated at 350 °C for 1 h reduced its irreversible capacity in the first cycle and facilitated capacity retention upon cycling (Fig. 8). On the other hand, oxidation at 500 °C resulted in a marked increased in irreversibility during the first discharge and in polarization between the charge and discharge branches; these changes reflect the adverse effect of an excessive oxygen content: incoming lithium atoms were trapped at irreversible and partially reversible links on particle surfaces.

Although oxidation by gases is difficult to control in terms of product reproducibility and uniformity [23], the

low cost of air-based procedures warrants attention for purposes such as the production of mass electrode materials. In fact, oxidation with air has proved an advantageous procedure for graphitic materials. The presence of a third site (Li bonded to armchair, zigzag or edge sites) may facilitate the observed increase in reversible capacity and decrease in irreversible capacity [24, 25]. The influence of the oxidation process on the electrochemical reaction of the original coke was found to depend on the strength of the treatment. Thus, polarization between charge and discharge curves was substantially increased when oxidation was done at 500 °C; this temperature, in addition, favoured irreversible formation of the SEI. By contrast, the samples treated at 350 and 400 °C exhibited more reversible galvanostatic profiles.

Figure 9 shows Nyquist plots for the original and oxidized cokes at the end of the first discharge. The overall impedance at the end of the first discharge was dependent on the particular treatment conditions used. Thus, the sample prepared by heating at 400 °C for 3 h exhibited a significant decrease in charge transfer resistance that was probably due to the formation of defects on particle surfaces; by contrast, it exhibited negligible changes in resistance of the SEI film. On the other hand, the sample obtained by heating at 500 °C for 3 h exhibited an abrupt increase in both resistance parameters.

The R_{SEI} value for the original coke increased abruptly in subsequent cycles (Fig. 10a), as previously found in other disordered carbon materials [26, 27]; this was a result of incomplete formation of the solid electrolyte interface after the first discharge. As the number of cycles increased, dispersion in the measured data increased to an extent precluding comparison among samples. SEI films formed on graphitized materials were previously found to be unstable by effect of their microexfoliation upon repeated cycling [28]. This phenomenon must continuously alter the morphology of the SEI film and lead to varying resistance values between successive cycles.

The variation of R_{CT} with the number of cycles showed more significant differences among the studied samples (Fig. 10b). Although the initial values were similar, the two parameters departed after the fifth cycle. Thus, the resistance values for the coke oxidized at 500 °C increased rapidly by effect of its poor capacity retention. By contrast, heating at 400 °C for 3 h proved the optimal treatment and provided a carbonaceous electrode material exhibiting a comparatively good kinetic response.

^{7}Li NMR spectroscopy is a useful technique for elucidating the mechanism of lithium insertion in carbonaceous materials [29–31]. Also, ^{7}Li MAS NMR spectroscopy could be of help to shed some light on the lithium reaction mechanism in these air-oxidized cokes. Figure 11 shows the spectra for electrodes discharged at 0.002 V and Table 3 lists the parameter values calculated from the deconvoluted spectra. The small signal at −0.94 ppm can be assigned to the presence of $LiPF_6$ incompletely removed

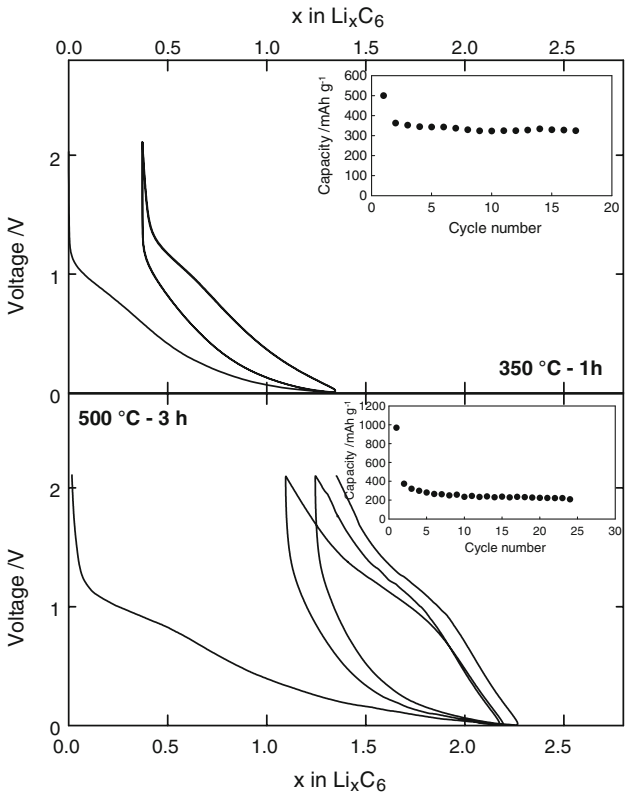

Fig. 8 Voltage versus composition plots of S1 coke oxidized at 350 °C—1 h and 500 °C—3 h. Inset: Capacity versus cycle number plot. Kinetic rate: C/10

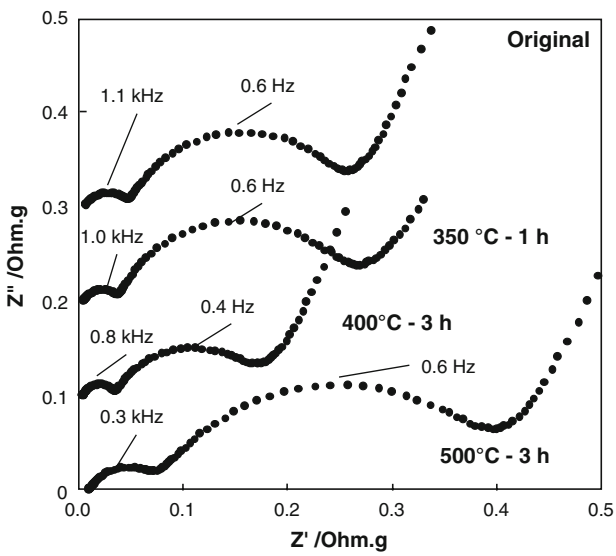

Fig. 9 Nyquist plots of three-electrode lithium cells assembled with untreated and oxidized S1 cokes as working electrodes. Spectra were recorded at the end of the first discharge

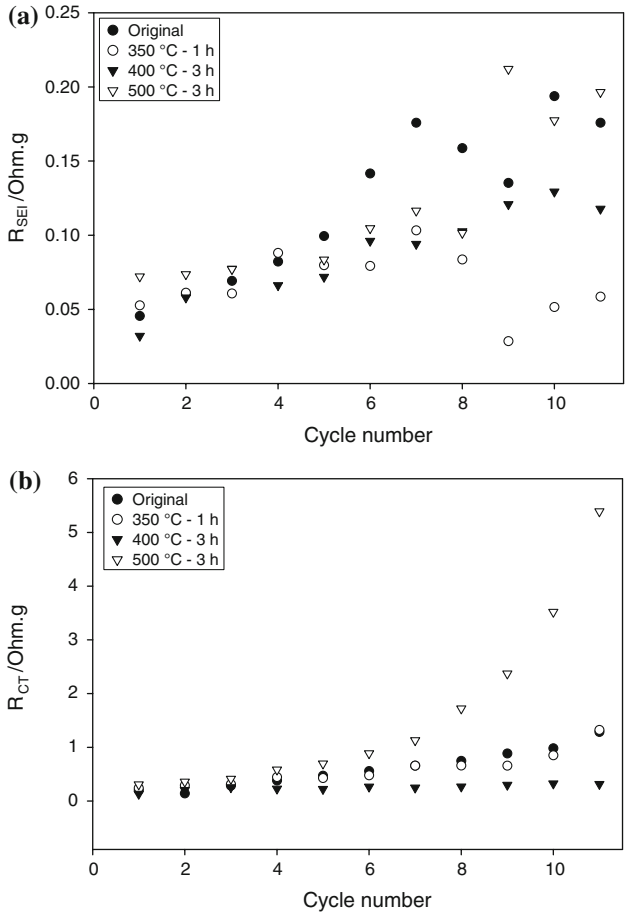

Fig. 10 Variation of resistance values versus cycle number of untreated and oxidized S1 cokes; **a** R_{SF} and **b** R_{CT}

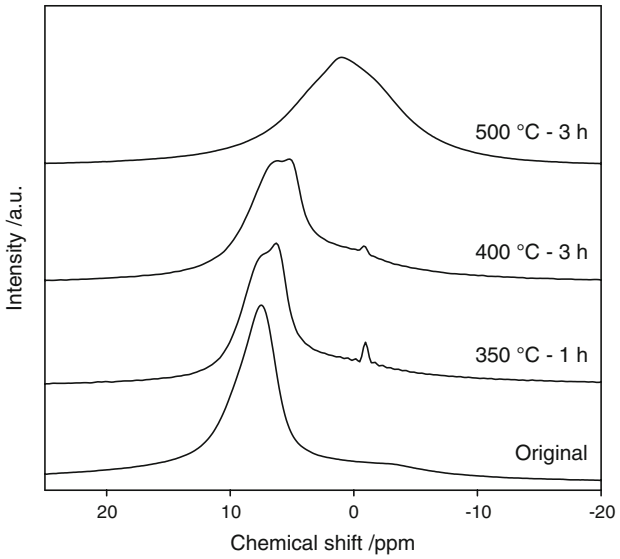

Fig. 11 ^{7}Li MAS NMR spectra of original and oxidized cokes at the end of the first discharge

Table 3 Chemical shift (CS), band width and contribution (C) values obtained from ^{7}Li MAS NMR spectra for original and oxidized S1 cokes

S1	CS (ppm)	Width (ppm)	C (%)
Original	−3.37	12.06	22.24
	0.93	2.18	1.08
	7.50	3.63	76.68
350 °C, 1 h	−0.94	0.83	1.60
	0.95	17.3	43.17
	6.17	1.89	20.56
	7.85	2.99	34.17
400 °C, 3 h	−0.78	0.98	1.04
	1.25	14.71	38.56
	5.0	1.48	8.39
	6.7	4.28	52.01
500 °C, 3 h	0.66	8.99	100

by rinsing. This signal rose over a highly broadened shoulder of the main peaks located at shifts slightly higher than 0 ppm. It is usually assigned to complex products from the electrolyte decomposition yielding the passivating layer the specific contributions of which cannot be resolved. Some authors have demonstrated the presence of $ROCO_2Li$, Li_2CO_3, ROLi and salt reduction products from FTIR spectra [16, 32, 33]. Several additional bands were observed at low-field values over the range 5–10 ppm. These new signals can be assigned to more covalently bonded lithium [34] which can be present between graphene particles in the interlayer space, and/or on the surface and at the edges of graphitic layers [31]. Chemical shifts decreased from the original coke to the highly oxidized sample, which reflects the ability of the new oxygenated surface groups to retain lithium atoms in ionic form. The most abrupt change in the spectral profile was observed upon raising the treatment temperature to 500 °C; the spectrum contained a single, broadened band at 0.66 ppm. Therefore, lithium atoms are exclusively bonded to surface ionic groups. The partial reversibility of these links is responsible for the high irreversibility, high polarization and poorer capacity retention of this material as compared with the samples treated at lower temperatures.

4 Conclusions

Petroleum cokes carbonized at 800 °C were subjected to mild oxidation with a stream of dry air under variable conditions. Irrespective of the particular coke, this treatment caused the irreversible capacity of the product to increase linearly with increasing heteroatom content. By contrast, capacity retention during long-term cycling was disparately influenced by the oxidation conditions. Thus,

the treatment was particularly efficient for coke S1 as it improved its electrochemical performance on cycling.

The oxidation treatment at 500 °C caused significant changes in the charge and discharge branches; also, it resulted in increased irreversibility during the first discharge and in high polarization. This was a consequence of lithium being trapped by oxygenated groups at particle surfaces. In fact, galvanostatic cycling at C/50 exposed substantial capacity fading. On the other hand, the cokes oxidized at 350 and 400 °C retained a high capacity value (as high as 385 mAh g^{-1} after 20 cycles in the coke treated at 350 °C for 1 h).

EIS measurements revealed an abrupt increase in charge transfer resistance in the sample treated at 500 °C for 3 h; the increase was correlated with its capacity fading. Therefore, an excessive oxygen content markedly increases the resistance of the material and hinders lithium migration across interfaces as a result.

Using ^{7}Li MAS NMR spectroscopy allowed us to shed new light on the nature of Li/carbon bonds in the studied electrodes. Thus, increasing the temperature and treatment time increased the ionic character of the bonds. For example, all lithium in the discharged electrode made from the sample treated at 500 °C was trapped by ionic links, probably at surface groups, which precluded reversible insertion between graphene layers.

Acknowledgements The authors are grateful to CICYT for financial support (contract MAT2005-00374 and contract MAT2001-1694) and M. C. Mohedano for her technical support. We thank SCAI (UCO Central Service for Research Support) and J. I. Corredor for the recording of the NMR spectra. R.A. is indebted to MCYT (Programa Ramón y Cajal). A. Concheso is indebted to MCYT for his predoctoral grant.

References

1. Nakajima T, Shibata S, Nagaa K, Ohzawa Y, Tressaud A, Durand E, Groult H, Warmont F (2007) J Power Sources 168:265
2. Kanga HG, Park JK, Hanc B-S, Lee H (2006) J Power Sources 153:170
3. Uono H, Kim B-C, Fuse T, Ue M, Yamaki J (2006) J Electrochem Soc 153(9):A1708
4. Alcántara R, Lavela P, Ortiz GF, Tirado JL, Stoyanova R, Zhecheva E, Jiménez-Mateos JM (2004) J Electrochem Soc 151(12):A2113
5. Alcántara R, Jiménez-Mateos JM, Tirado JL (2002) J Electrochem Soc 149:A201
6. Concheso A, Santamaría R, Granda M, Menéndez R, Jiménez-Mateos JM, Alcántara R, Lavela P, Tirado JL (2005) Electrochim Acta 50:1225
7. Machnikowski J, Frackowiak E, Kierzek K, Waszak D, Benoit R, Béguin F (2004) J Phys Chem Solids 65:153
8. Balan L, Schneider R, Billaud D, Ghanbaja J (2005) Mater Lett 59:1080
9. Concheso A, Santamaría R, Blanco C, Menéndez R, Jiménez-Mateos JM, Alcántara R, Lavela P, Tirado JL (2005) Carbon 43:923
10. Zhao H, Ren J, He X, Li J, Jiang C, Wan C (2007) Electrochim Acta 52:6006
11. Gao J, Zhang HP, Fu LJ, Zhang T, Wu YP, Takamura T, Wu HQ, Holze R (2007) Electrochim Acta 52:5417
12. Wu YP, Jiang C, Wan C, Holze R (2002) J Appl Electrochem 32(9):1011
13. Shim J, Striebel KA (2007) J Power Sources 164:862–867
14. Wu YP, Holze R (2003) J Solid State Eletrochem 8:73
15. Concheso A, Santamaría R, Menéndez R, Jiménez-Mateos JM, Alcántara R, Lavela P, Tirado JL (2006) Electrochim Acta 52:1281
16. Aurbach D, Markovsky B, Weissman I, Levi E, Ein-Eli Y (1999) Electrochim Acta 45:67
17. Jiang W, Tran T, Song X, Kinoshita K (2000) J Power Sources 85:261
18. Wu YP, Rahm E, Holze R (2002) Electrochim Acta 47:3491
19. Larcher D, Mudalige C, Gharghouri CM, Dahn JR (1999) Electrochim Acta 44:4069
20. Concheso A, Santamaría R, Blanco C, Menéndez R, Jiménez-Mateos JM, Gómez García FJ, Alcántara R, Lavela P, Tirado JL (2007) Carbon 45:1396
21. Zaghib K, Song X, Kinoshita K (2001) Thermochim Acta 371:57
22. Wang C, Appleby AJ, Little FE (2002) J Electroanal Chem 519:9–17
23. Fu LJ, Liu H, Li C, Wu YP, Rahm E, Holze R, Wu HQ (2006) Solid State Sci 8:113
24. Peled E, Menachem C, Melman A (1996) J Electrochem Soc 143:L4
25. Menachem C, Wang Y, Flowers J, Peled E, Greenbaum SG (1998) J Power Sources 76:180
26. Concheso A, Santamaría R, Menéndez R, Alcántara R, Lavela P, Tirado JL (2006) J Power Sources 161:1324
27. Concheso A, Santamaría R, Menéndez R, Jiménez-Mateos JM, Alcántara R, Lavela P, Tirado JL (2006) Carbon 44:1762
28. Aurbach D, Markovsky B, Levi MD, Levi E, Schechter A, Moshkovich M, Cohen Y (1999) J Power Sources 81–82:95
29. Sato K, Noguchi M, Demahi A, Oki N, Endo M (1994) Science 264:556
30. Conard J, Lauginie P (2000) Tanso 191:62
31. Wang S, Matsui H, Taamamura H, Matsamura Y, Yamabe T (1998) Phys Rev B 58:8163
33. Aurbach D, Gnanaraj JS, Levi MD, Levi EA, Fischer JE, Claye A (2001) J Power Sources 97–98:92
34. Ein-Eli Y, Markovsky B, Aurbach D, Carmeli Y, Yamin H, Luski S (1994) Electrochim Acta 3:2559
35. Dai Y, Wang Y, Eshkenazi V, Peled E, Greenbaum SG (1998) J Electrochem Soc 145:1179